

Nondeterministic Nagel-Schreckenberg traffic model with open boundary conditions

S. Cheybani,^{1,2} J. Kertész,^{2,3} and M. Schreckenberg¹¹Theoretische Physik, Gerhard-Mercator Universität, D-47048 Duisburg, Germany²Department of Theoretical Physics, Technical University of Budapest, H-1111 Budapest, Hungary³Laboratory of Computational Engineering, Helsinki University of Technology, FIN-02150 Espoo, Finland

(Received 26 April 2000; published 20 December 2000)

We study the phases of the Nagel-Schreckenberg traffic model with open boundary conditions as a function of the randomization probabilities $p > 0$ and the maximum velocity $v_{max} > 1$. Due to the existence of “buffer sites” which enhance the free-flow region, the behavior is much richer than that of the related, parallel updated asymmetric exclusion process [(ASEP), $v_{max} = 1$]. Such sites exist for $v_{max} \geq 3$ and $p < p_c$ where the phase diagram is qualitatively similar to the $p = 0$ case: there is a free flow and a jamming phase separated by a line of first-order transitions. For $p > p_c$ an additional maximum current phase separated by second-order transitions occurs like for the ASEP. The density profile decays in the maximum current phase algebraically with an exponent $\gamma \approx \frac{2}{3}$ for all $v_{max} \geq 2$ indicating that these models belong to another universality class than the ASEP where $\gamma = \frac{1}{2}$.

DOI: 10.1103/PhysRevE.63.016108

PACS number(s): 05.40.-a, 45.70.Vn

I. INTRODUCTION

Asymmetric exclusion processes (ASEP) play an important role in nonequilibrium statistical mechanics. The one-dimensional ASEP is a lattice model which describes particles hopping in one direction with stochastic dynamics and hard core exclusion. It was introduced in 1968 to provide a qualitative understanding of the kinetics of the protein synthesis on ribonucleic acid (RNA) templates [1]. It turned out, however, that—despite its simplicity—there are numerous further applications of the ASEP on the field of interface growth, polymer dynamics, and traffic flow [2–6].

Unfortunately, as far as traffic is concerned, the ASEP yields rather unrealistic results, because essential phenomena like acceleration or slowing down cannot be reproduced in this model. As a consequence, Nagel and Schreckenberg developed an extension of the ASEP resulting in a one-dimensional probabilistic cellular automaton model [5]. According to the Nagel-Schreckenberg model the road consists of a single lane which is divided into L cells of equal size numbered by $i = 1, 2, \dots, L$ and the time is also discrete. Each site can be either empty or occupied by a car with integer velocity $v = 0, 1, \dots, v_{max}$. All sites are simultaneously updated according to four successive steps.

- (1) Acceleration: increase v by 1 if $v < v_{max}$.
- (2) Slowing down: decrease v to $v = d$ if necessary (d is the number of empty cells in front of the car).
- (3) Randomization: decrease v by 1 with randomization probability p if $p > 0$.
- (4) Movement: move car v sites forward.

Either ring (periodic boundary conditions) or open (open boundary conditions) geometry is considered. In the case of ring geometry cars move on a ring and the car density in the system keeps constant. Open systems, on the other hand, are characterized by the injection (extinction) rate α (β), which means by the probability α (β) that a car moves into (out of) the system.

For the maximum velocity $v_{max} = 1$ the model is identical

with the ASEP with parallel update [7–9] which has been solved exactly with periodic boundary conditions [6] and recently also with open boundary conditions [9,10]. In this special case three regimes (free flow, jamming, and maximum current) can be distinguished from each other. The transition from the free flow to the jamming phase at the $\alpha = \beta$ line for $\alpha, \beta < 1 - \sqrt{p}$ is of first order. The transition from the free flow (jamming) to the maximum current phase is continuous and takes place at the injection (extinction) rate α_c (β_c) with $\alpha_c(p) = \beta_c(p) = 1 - \sqrt{p}$. The adequate scheme for traffic simulations is parallel updating [11] and this is applied also in the Nagel-Schreckenberg model. Systems with parallel update are, furthermore, characterized by strong short-range correlations, and therefore, short-range correlation functions play an important role here [12,24].

Most of the work dealing with the Nagel-Schreckenberg model for $v_{max} > 1$ impose periodic boundary conditions [13–24]. Much attention has been paid to the question of the transition from the free flow to the jamming regime. According to the state-of-the-art this is a crossover rather than a sharp transition [16–25]. Systems with periodic boundary conditions are, furthermore, characterized by a trivial density profile $\rho(i) = \rho$ with $1 \leq i \leq L$ due to translational invariance. In this context it should be mentioned that short-range correlation functions are well suited for the description of the free-flow–jamming transition [24]: The free-flow regime is characterized by anticorrelations around a propagating peak, that is, in free flow cars are surrounded by empty space. At the critical density ρ_c the anticorrelations are maximally developed, and for higher densities they vanish. Simultaneously, a jamming peak develops according to the fact that the back car is strongly slowed down in a jam. In the following, systems for maximum velocities $v_{max} \leq 10$ are investigated for the more realistic case of open boundaries. Boundary conditions are defined as in [26]: At site $i = 0$, which means out of the system a vehicle with the probability α and with the velocity $v = v_{max}$ is created. This car immediately moves according to the Nagel-Schreckenberg rules. If the velocity of the injected car on $i = 0$ is $v = 0$ (because site i

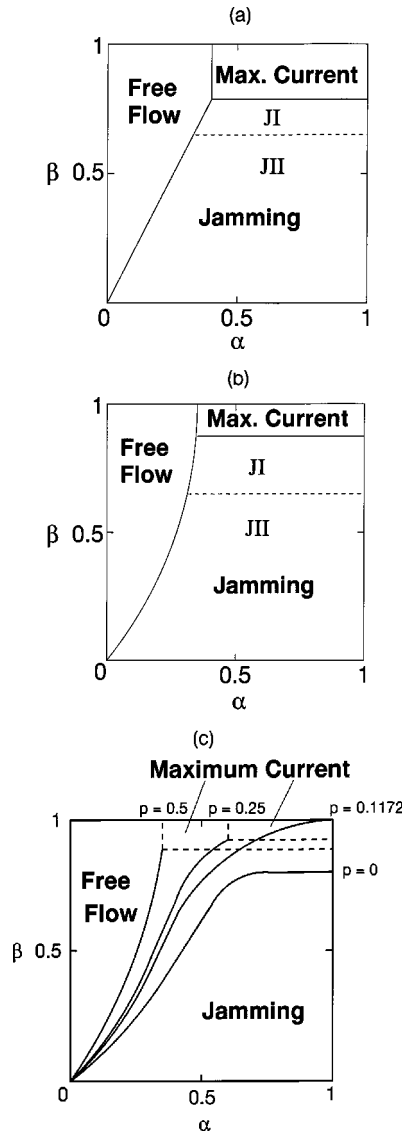


FIG. 1. (a) Phase diagram for $v_{max}=2$ ($p=0.5$, continuous line: first-order or continuous-phase transition; dotted line: border between AI-AII and BI-BII; broken line: border between the JI and the JII regime). Although there is no symmetry along the $\alpha=\beta$ line the phase diagram shows strong similarities to the $v_{max}=1$ case. (b) Phase diagram for $v_{max} \geq 5$ ($p=0.5$, continuous line: first-order or continuous-phase transition; dotted line: border between AI-AII and BI-BII; broken line: border between the JI and the JII regime). Phase diagrams for $v_{max}=3, 4$ are qualitatively the same. Due to the buffer effect the border between the free flow and the jamming phase shows a slight bending. (c) Phase diagram for $v_{max}=5$ and $p=0, 0.1172, 0.25$, and 0.5 . For randomization probabilities $p > p_c$ with $p_c=0.1172 \pm 0.008$ the buffer effect vanishes and the free-flow regime becomes smaller with increasing randomization probability. The borders of the maximum current regime for $\alpha > 0.6$, $\beta > 0.92$, and $p=0.25$ ($\alpha > 0.35$, $\beta > 0.89$, and $p=0.5$) are represented by broken lines. The phase diagram for maximum velocities $v_{max} > 5$ is very similar.

$=1$ is occupied by another car or because the front car is on site $i=2$ and the injected car is slowed down by 1 due to randomization) then the injected car is deleted. At $i=L+1$ a “block” occurs with probability $1-\beta$ and causes a slowing

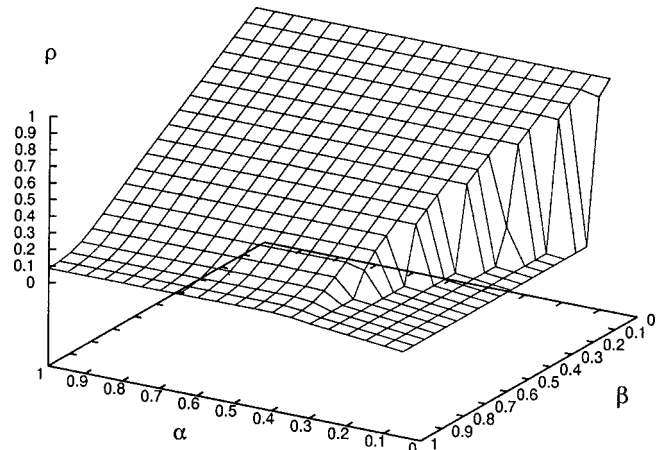


FIG. 2. Average density in the middle of the system for $v_{max}=5$ ($p=0.5$). The first-order phase transition from freely moving to jammed traffic can be clearly seen. Moreover, there is a jump in the derivative of $\rho(i, L/2)$ at the maximum current-free flow and the maximum current-jamming border which is a hint of a continuous-phase transition.

down of the cars at the end of the system. Otherwise, with probability β , the cars simply move out of the system. In [26] systems with open boundaries have been already analyzed for the randomization probability $p=0$, i.e., by ignoring the randomization step. The most interesting feature of the deterministic Nagel-Schreckenberg (NS) model for maximum velocities $v_{max} \geq 3$ and open boundaries is the existence of so-called buffers: As a consequence of the parallel updating and the hindrance an injected car feels from the front car at the beginning of the system spaces larger than v_{max} develop between two neighboring cars for high injection rates. This can be easily demonstrated by considering $i=0$ and the first sites of the system $i=1, \dots, 5$ for $\alpha=\beta=1$ and $v_{max} \geq 3$. At an arbitrary time $t=t_0$ a car with velocity v_{max} is injected on $i=0$, i.e.,

injection: $v_{max}| \dots 2 \dots$

After application of the NS rules on the system we have injected on $i=0$, i.e.,

movement: $\dots | 2 \dots \dots$

Correspondingly, we get for $t=t_0+1$

injection: $v_{max}| \dots 2 \dots \dots$

movement: $\dots | 1 \dots \dots 3$

and for $t=t_0+2$

injection: $v_{max}| 1 \dots \dots 3$,

movement: $0 | \dots 2 \dots \dots$

As the car on site $i=0$ cannot move it is deleted and the situation starts over in the next time step,

injection: $v_{max}| \dots 2 \dots \dots$,

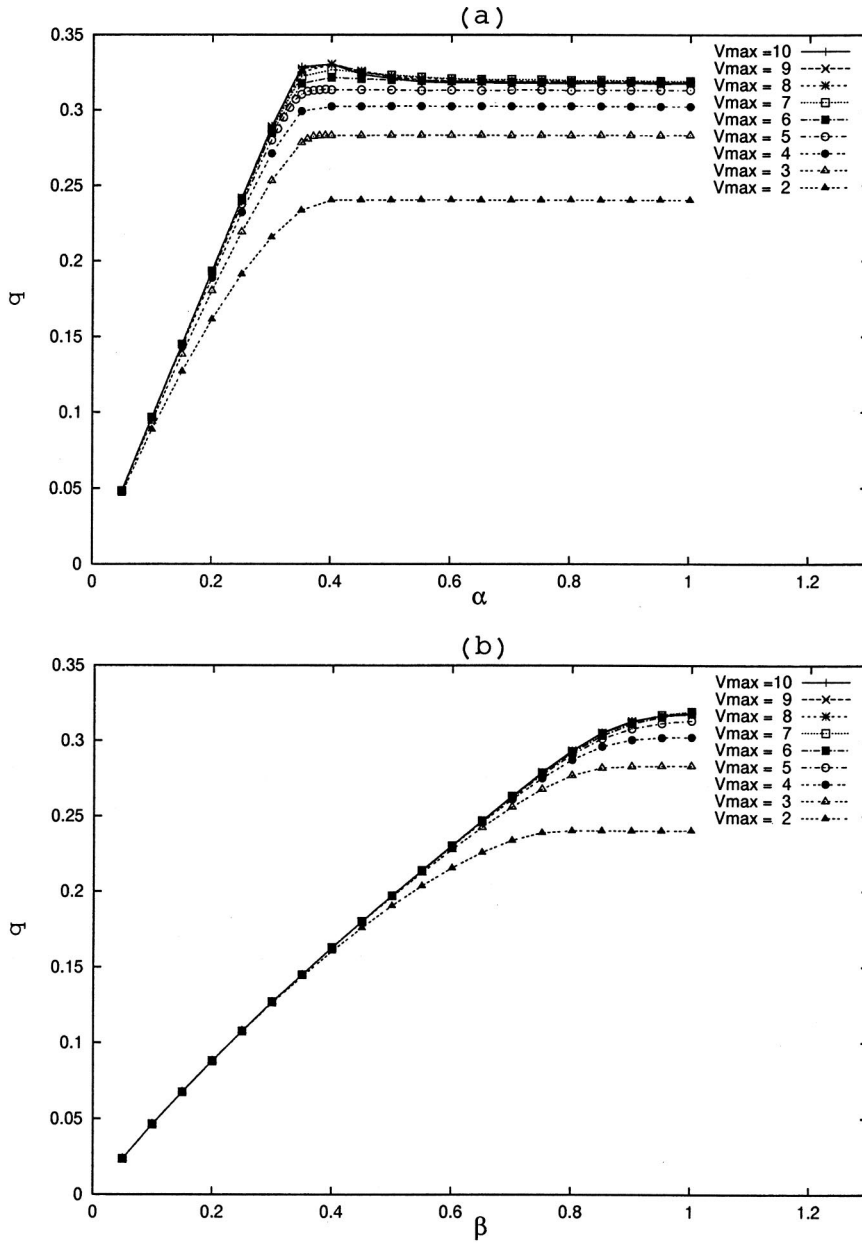


FIG. 3. (a) Current q for $v_{max} = 2, 3, \dots, 10$ and $\beta = 1$ ($p = 0.5$). At $\alpha \approx 0.35$ there is a slight maximum for $v_{max} \geq 5$ which is explained in Fig. 4(a). (b) Current q for $v_{max} = 2, 3, \dots, 10$ and $\alpha = 1$ ($p = 0.5$). For $v_{max} \geq 5$ the curves are identical.

movement: $\dots | 2 \dots ,$

and so on. Obviously, one car is lost out of three injection possibilities. In the system, far from the boundaries, the distance between two neighboring cars turns out to be alternately $d_1 = v_{max}$ and $d_2 = 2(v_{max} - 1)$. That means, in addition to the expected v_{max} empty sites larger gaps occur in the $\alpha \rightarrow 1$, $\beta \rightarrow 1$ limit. We call these additional sites ‘‘buffers’’ because they have a buffer effect at the end of the system: Due to these sites the development of jamming waves is suppressed even for $\beta < 1$. The transition from the free flow to the jamming phase is of first order and accompanied by the collapse of the buffers. The effect resulting from the buffers does not depend on the maximum velocity if $v_{max} \geq 5$ (for $v_{max} = 3, 4$ the buffer effect is not so strong as the buffers are not completely developed for that case).

However, randomization is indispensable for the analysis of real traffic as it takes human behavior into account: The behavior of a car driver is not like that of a machine but rather contains unpredictable elements. In traffic, over-reactions when slowing down can be found as well as delays when accelerating; furthermore, there are fluctuations when following a car (follow-the-leader situation) and so on.

Besides this motivation it is of interest to compare the general $p > 0$, $v_{max} \geq 1$ case with the previously investigated models ($p > 0$, $v_{max} = 1$ [9,10] and $p = 0$, $v_{max} \geq 1$ [26]). The presented results were obtained by simulating a $L = 1024$ sample with at least 1000 runs with 10^4 time steps each. In order to investigate the influence of randomization on the system we proceed similarly to [26]: Section II considers the behavior of the current and average occupation number in the middle of the system. Section III deals with density profiles, Sec. IV with short-range

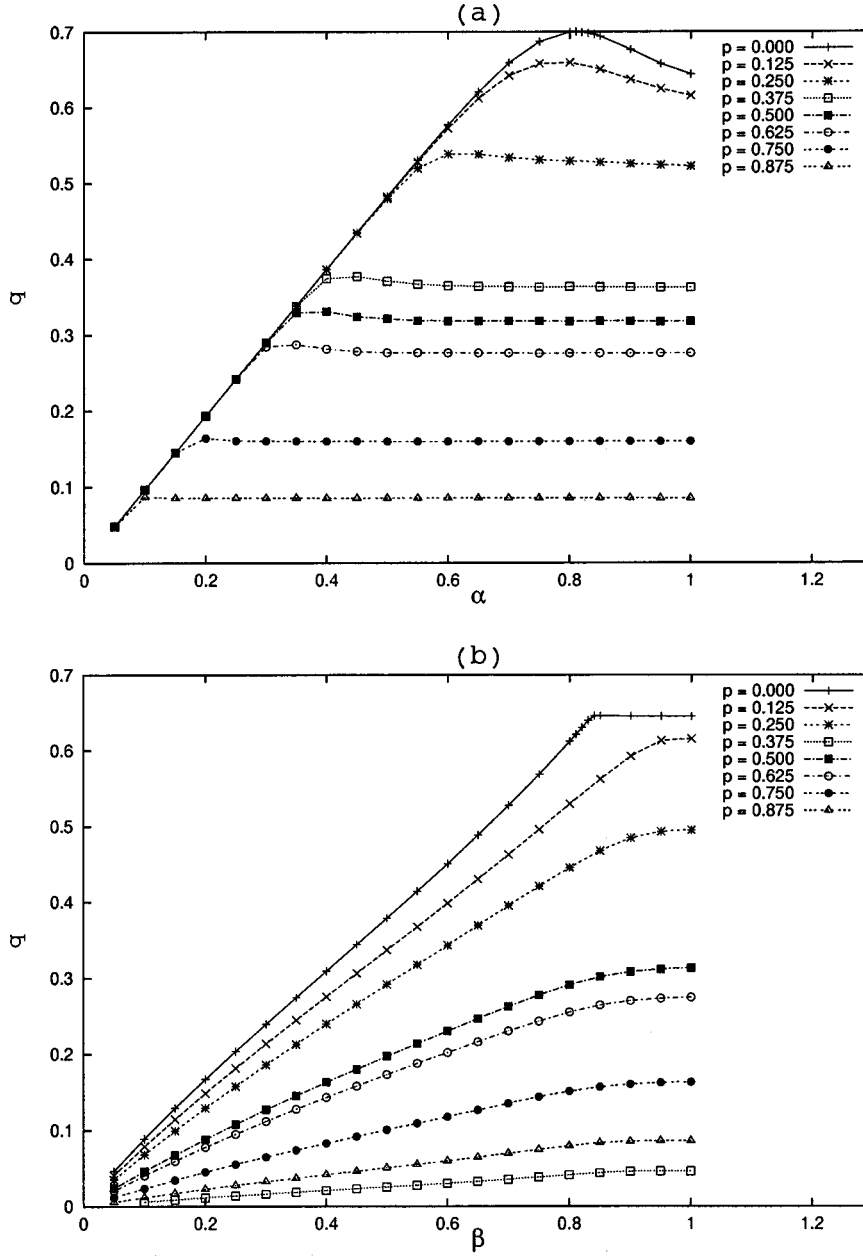


FIG. 4. (a) Current q for $p = 0, 0.125, \dots, 0.875$ and $\beta=1$ ($v_{max}=10$). The maximum at $\alpha \approx 0.81$ for $p=0$ moves towards smaller injection rates with increasing randomization probabilities and for $p > 0.125$ a continuous-phase transition is observed. (b) Current q for $p=0, 0.125, \dots, 0.875$ and $\alpha=1$ ($v_{max}=5$). For $p > 0$, the buffer effect observed for the deterministic case vanishes and the first-order phase transition goes over into a continuous-phase transition.

correlation functions. Finally, the results are summarized in Sec. V.

II. CURRENT AND AVERAGE OCCUPATION NUMBER AT THE MIDDLE OF THE SYSTEM

The phase diagram for systems with probability $p=0.5$ and maximum velocity $v_{max}=2$ and $v_{max} \geq 5$ is shown in Figs. 1(a) and 1(b) (the case $v_{max}=3,4$ is similar to the latter case). For $v_{max}=2$ the phase diagram [Fig. 1(a)] is qualitatively the same as for the case $v_{max}=1$ [9,10]: The free flow and the jamming regime are divided by a straight line and for $\alpha > 0.35$ and $\beta > 0.8$ the system is in the maximum current phase. Obviously, the maximum current regime is smaller than for $v_{max}=1$ and there is no symmetry along the $\alpha=\beta$ line. For $v_{max}=3$ the maximum current regime is even smaller (for $\alpha > 0.35$ and $\beta > 0.85$) and the free-flow–

jamming border shows a slight bending. These tendencies are even stronger developed for higher maximum velocities v_{max} with a maximum current regime for $\alpha > 0.35$, $\beta > 0.87$, and $v_{max}=4$ [for $\alpha > 0.35$ and $\beta > 0.89$, and $v_{max} \geq 5$, see Fig. 1(b)].

Another interesting feature of the nondeterministic case is that the course of the free-flow–jamming border is totally different from that for $p=0$. In Fig. 1(c) it can be clearly seen that this difference is a consequence of the vanishing buffer effect due to randomization. For randomization probabilities $p > p_c$ ($p_c = 0.1172 \pm 0.008$ for $v_{max}=5$) there is no sign of the buffer effect any more, and a (rectangular) maximum current regime develops for $\alpha > \alpha_{FreeFlow}$ and $\beta > \beta_{Jamming}$.

In order to understand the nature of the transition between the phases we consider the average occupation number on the site $i=L/2$, ρ ($i=L/2$), as proposed in [8]. Figure 2

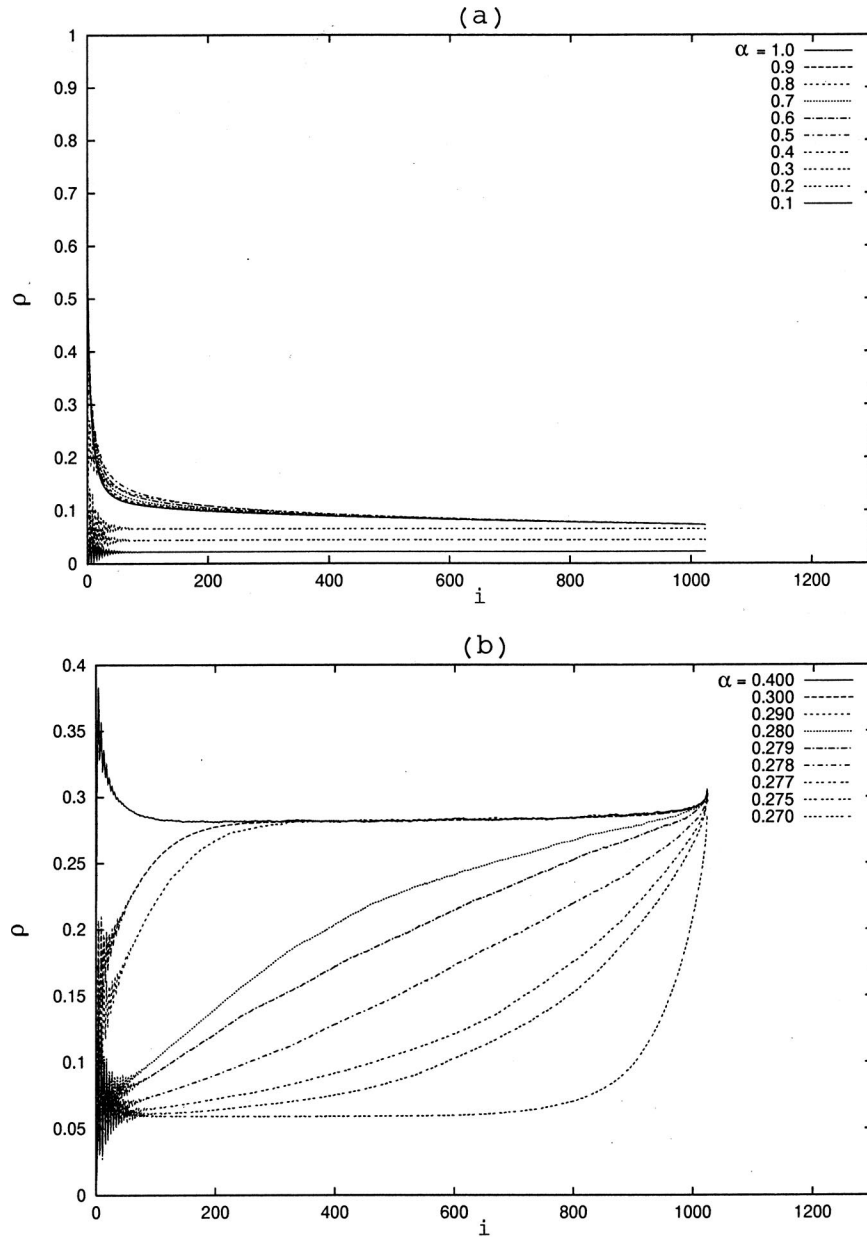


FIG. 5. (a) Density profiles for $\beta=1$ ($p=0.5$, $v_{max}=5$). A typical feature of density profiles in the free-flow regime is oscillations resulting from the hindrance the cars have at the beginning of the system from each other. These oscillations die out for higher system sites due to randomization. The curves decay algebraically in the maximum current regime as it is already known from the ASEP. (b) Density profiles for $\beta=0.7$ ($v_{max}=5$, $p=0.5$). The phase transition at $\alpha=0.278$ is of first order characterized by a linear density profile at the critical injection rate. The curve for $\alpha=0.4$ ($\alpha=0.3$ or $\alpha=0.29$) is typical for a density profile in the BII (BI) regime. (c) Density profiles for $\alpha=1$ ($p=0.5$, $v_{max}=5$). The results from the $v_{max}=1$ case are recovered: In the maximum current regime ($\beta>0.89$) the density profiles decay algebraically and in the BII jamming regime they are described by an enhanced exponential function.

shows ρ ($i=L/2$) for $v_{max}=5$ as a function of the injection and the extinction rates (the average occupation number on $i=L/2$ for any $v_{max}>1$ behaves similarly). It turns out that phase transitions in systems with maximum velocity $v_{max}>1$ show the following features: The transition from free flow to jamming is of first order indicated by a jump in ρ ($i=L/2$). At the maximum current-free flow and the maximum current-jamming transition there is a jump in the derivative of ρ ($i=L/2$) which is a hint at a continuous-phase transition. These conclusions will be confirmed in Sec. III

which deals with the investigation of the corresponding density profiles.

In the following we analyze the current due to the influence of the boundaries, maximum velocity v_{max} , and randomization probability p . The best way to investigate the influence of the left boundary is to consider the case $\beta=1$ for $p=0.5$ where cars simply move out of the system. In Fig. 3(a) free flow and maximum current phase can be clearly distinguished from each other. For maximum velocities $v_{max}\geq 5$ the curves are nearly the same with a maximum at

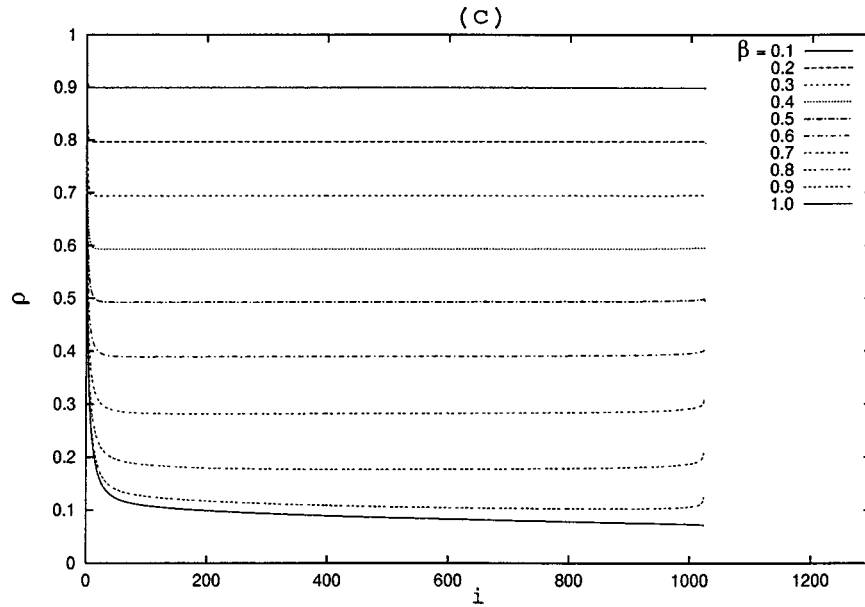


FIG. 5 (Continued).

$\alpha \approx 0.35$ becoming stronger with increasing v_{max} (the occurrence of the maximum will be explained below). The dependence of the current on α and β for $v_{max}=2, 3, 4$ is qualitatively the same as for $v_{max}=1$. For the investigation of the influence of the right boundary we consider the case $\alpha=1$ for $p=0.5$ [Fig. 3(b)]. Here, the current for $v_{max} \geq 5$ does not depend on the maximum velocity. Furthermore, it seems to increase monotonously with increasing β also in the maximum current phase ($\beta > 0.89$). Investigations for system sizes $L \geq 4096$, however, show that the latter observation is just a finite size effect and that the current for $v_{max} \geq 5$ and $\beta > 0.89$ is constant. Apart from this, the curves for the current do not change in an essential way with increasing system size L , and therefore it is sufficient to investigate systems with $L=1024$ in the following.

From the observations so far we can conclude that—as for the deterministic case—the behavior of the system only negligibly changes when maximum velocities $v_{max} \geq 5$ are considered. Therefore we restrict ourselves to the case $v_{max}=5$ in the following observations.

We will now investigate the influence of the randomization probability on the behavior of the system. It can be seen from Figs. 4(a) and 4(b) that the buffer effect observed for the deterministic case vanishes with increasing p : For $\beta=1$ in Fig. 4(a) the maximum at $\alpha \approx 0.81$ resulting from the existence of the buffers moves to the left and becomes weaker and weaker. [In Fig. 4(a) we make an exception and consider the current at $v_{max}=10$ instead of $v_{max}=5$, because for the latter case this effect is nearly invisible.] For the injection rate $\alpha=1$, on the other hand, the buffer effect vanishes as soon as randomization probabilities $p > p_c$ are considered.

To sum up it can be said that as a consequence of the buffer effect, the course of the current in the maximum current phase deviates from the expected (constant) behavior for $\beta=1$, $p=0.5$, and maximum velocities $v_{max} \geq 5$ showing a slight maximum at $\alpha \approx 0.35$. Besides, there are strong indications that a continuous transition from the free flow (jam-

ming) to a maximum current phase develops with increasing randomization probability on the $\beta=1$ line ($\alpha=1$ line). More convincing arguments for the existence of a maximum current phase, however, will be given in the following sections.

III. DENSITY PROFILES

Our observations so far consider the behavior of the whole system and of the site $i=L/2$. For the analysis of what happens on the other sites it is useful to investigate the density profiles. Of special interest in this context is the question in how far the density profiles reflect the transition between the phases. For that purpose we consider the density profiles for $\beta=1$ (\rightarrow transition from free flow to maximum current), for $\beta=0.7$ (\rightarrow transition from free flow to jamming), and for $\alpha=1$ (\rightarrow transition from maximum current to jamming). It turns out that—as in the case of $v_{max}=1$ —the free-flow (jamming) phase can be divided into the regime AI and AII (BI and BII). The following investigations are confined to the randomization probability $p=0.5$, $L=1024$, and $v_{max}=5$ (for $v_{max} \geq 5$ and $L > 1024$ the density profiles are qualitatively the same).

In Fig. 5(a) the transition from free flow to maximum current for $\beta=1$ can be clearly seen. The free-flow regime is characterized by oscillations at the beginning of the system dying out for $i \geq 100$ (if $p=0.5$ and $v_{max}=5$) due to randomization and the density profile becomes constant. It can therefore be said that randomization blurs the influence of the left boundary. In the maximum current regime we do not have any oscillations at all. Instead, an analytic decrease of the density is observed becoming stronger with increasing α . This phenomenon can be easily understood as cars hinder each other at the beginning of the system for high injection rates: The higher the injection rate the stronger the hindrance. As a consequence the density profiles in the maximum current phase do not depend at all on α in the middle

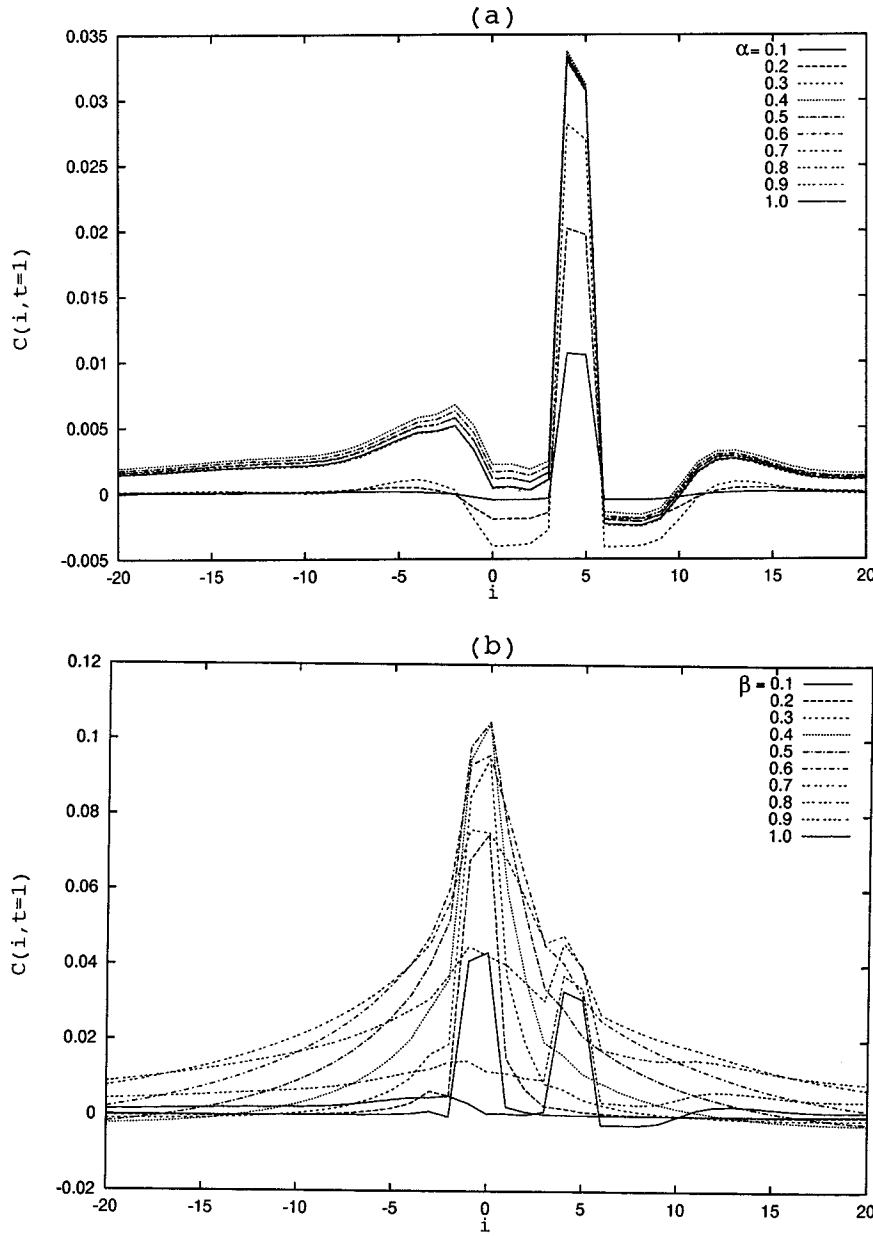


FIG. 6. (a) Correlation functions for $\beta=1$ ($p=0.5$, $v_{max}=5$). The free-flow regime is characterized by a propagating peak with anticorrelations around it. In the coexistence regime both the jamming and the propagating peak can be observed. (b) Correlation functions for $\alpha=1$ ($p=0.5$, $v_{max}=5$). The curves in the maximum current and in the JI jamming regime behave similarly. At $\beta \approx 0.75$ the propagating peak vanishes and the system is in the JII jamming (“superjamming”) regime. (c) Correlation functions for $\beta=1-\alpha$ ($p=0.5$, $v_{max}=5$). As for the injection rate $\alpha=1$, the propagating peak vanishes at $\beta=1-\alpha \approx 0.75$. Moreover, there is a striking similarity to corresponding correlation functions in the case of periodic boundary conditions.

and at the end of the system. At the beginning of the system, however, the density profiles decay as $i^{-\gamma}$ with $\gamma \approx 0.66$ which is valid for all $v_{max} > 1$. We conjecture that $\gamma = \frac{2}{3}$ because the exponent converges to this value with increasing system sizes. That means that the cases $v_{max}=1$ and $v_{max} > 1$ belong to different universality classes since the corresponding density profiles for the ASEP with parallel update decay as $i^{-\gamma}$ with $\gamma = \frac{1}{2}$ at the beginning of the system [9,10].

The free-flow–maximum current transition is nicely reflected by the density at the end of the system: $\rho(i=L)$ is

proportional to the injection rate when the cars move freely up to $\alpha_c = 0.35$ and becomes constant in the maximum current regime. The situation is different when density profiles at the free-flow–jamming border for $\beta=0.7$ are considered [Fig. 5(b)]. It can be easily seen that the transition is of first order as the density profile at $\alpha_c = 0.278$ is linear which is a typical feature of a first-order phase transition (see [11] and references therein).

The density profiles for the injection rate $\alpha=1$ are shown in Fig. 5(c). The course of the curves for $\beta < 0.89$ ($\beta > 0.89$) is typical for the maximum current (BII jamming)

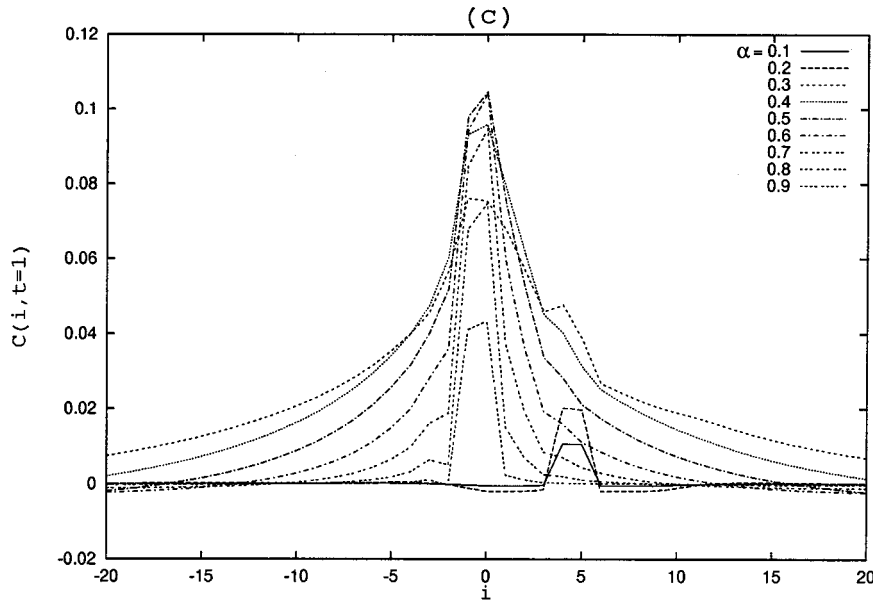


FIG. 6 (Continued).

phase with an algebraic (exponential) decay at the beginning of the system due to the hindrance already described for $\beta = 1$. The decay becomes weaker with decreasing β and finally vanishes as the repercussion resulting from the blockage at $i=L+1$ increasingly superimposes the hindrance effect at the beginning of the system. For extinction rates $0.6 \leq \beta \leq 0.9$ there is a slight increase at the end of the system which indicates a hindrance due to the blockage. It just remains a border effect, however, and is of no relevance for the considerations in this paper.

IV. CORRELATION FUNCTIONS

In this chapter we consider short-range correlation functions

$$C(i, t) = \langle \eta(i', t') \eta(i+i', t+t') \rangle_{i', t'} - \langle \eta(i', t') \rangle_{i', t'}^2,$$

where

$$\eta(i', t') = 1 \quad \text{if site } i' \text{ is occupied at time } t'$$

$$\eta(i', t') = 0 \quad \text{else.}$$

$\langle \dots \rangle_{i', t'}$ describes the spatial and temporal average over all L sites i' and over times t' taken from our simulation of the steady state. The correlation functions are measured in the middle of the system where the influence of the boundaries is minimal. We do not only investigate the cases $\beta=1$ [influence of the left boundary, Fig. 6(a)] and $\alpha=1$ [influence of the right boundary, Fig. 6(b)], but also $\beta=1-\alpha$ [Fig. 6(c)]. For the latter case there are similar conditions at both boundaries and the system can be compared at best with the corresponding system with periodic boundary conditions. Therefore it is no surprise that the correlation functions in Fig. 6(c) are qualitatively the same as those for periodic boundary conditions [24].

What is interesting, however, is that a classification into free flow, maximum current, and jamming cannot be done when short-range correlation functions are considered. Instead, due to Figs. 6(a)–6(c) three regimes can be distinguished from each other

(a) *Free flow*. The free flow is characterized by anticorrelations around a propagating peak at $i=v_{max}(t-1)$ with a shoulder at $i=v_{max}t$, that is, in free flow moving cars are surrounded by empty space.

(b) *Coexistence regime (JI + maximum current)*. The coexistence of free flow and jamming manifests itself in the double-peak structure of the correlation function. The jamming causes a maximum at $i=-1$ according to the hindrance the back car feels in the jam.

(c) *Jamming II (JII, ‘superjamming’)*. The propagating peak disappears as a consequence of the fact that in free flow moving cars do not exist any longer.

As is obvious from the previous sections the transition from JI to JII is not a phase transition and does not change the behavior of the system in an essential way. In correspondence with [24] the critical injection (extinction) rate α_{c2} (β_{c2}) for the JI-JII transition is defined by the vanishing of the propagating peak and takes place at $\beta_{c2} \approx 0.65$ [see also Fig. 1(b)]. Unfortunately, an exact value for the free-flow–jamming transition can neither be given. As a consequence of the randomized oscillations in the density at the beginning of the system it is not possible to determine the critical injection (extinction) rate at which the influence of the right boundary reaches the left boundary. This is a significant difference to the deterministic case [26] where the oscillations of the free-flow phase form a well-defined pattern due to the lack of randomization.

The transition from jamming I to jamming II takes place at $\beta \approx 0.65$ for all $v_{max} > 1$. In other words: When the maximum velocity is varied free flow, JII, and the coexistence

phase (JI+maximum current) keep constant and only the ratio between the maximum current phase and JI changes [Figs. 1(a) and 1(b)].

V. CONCLUSIONS

The nondeterministic Nagel-Schreckenberg model with open boundaries depends on the randomization, the maximum velocity, and the boundary conditions. The buffer effect observed for the deterministic case $p=0$ and $v_{max} \geq 3$ is strongly weakened with increasing randomization probability. For $v_{max}=2$ there are no buffers and therefore the corresponding phase diagram is similar to the case $v_{max}=1$ for all p values. For $v_{max} \geq 3$ and $p > p_c$ ($p_c = 0.1172 \pm 0.008$ for $v_{max}=5$) the buffer effect completely vanishes since the development of jamming waves is no longer suppressed. As a consequence, a maximum current phase occurs for $p > p_c$ and the free-flow (jamming) phase can be divided into two regimes AI and AII (BI and BII) similarly to the case of $v_{max}=1,2$. Another analogy to the case $v_{max}=1$ is that the free-flow–jamming (free-flow–maximum current and jamming–maximum current) transition is of first (second) order.

There are, however, essential differences between systems with $v_{max}=1$ and $v_{max} > 1$: In the maximum current phase the density profiles decay algebraically with an exponent γ

$=\frac{2}{3}$ for $v_{max} \geq 2$ whereas $\gamma=\frac{1}{2}$ was obtained in the ASEP. This indicates that systems with $v_{max} > 1$ and $v_{max}=1$ belong to different universality classes. Another difference to the ASEP is the existence of oscillations at the beginning of the system due to the repulsion of the cars.

The comparison of systems with periodic and with open boundary conditions suggests that there are mainly three differences. First of all, the transition from free flow to jamming for systems with open boundaries is sharp and there is no maximum current phase in the case of periodic boundary conditions. Moreover, the dependence on the maximum velocity is more complex for systems with open boundary conditions due to the occurrence of the buffers. However, there are common features, too: Measurements of the short-range correlation function show that, as for corresponding systems with periodic boundary conditions, three regimes can be distinguished from each other: (a) free flow: cars do not hinder each other; (b) maximum current and jamming I: coexistence of freely moving and jammed cars; (c) jamming II: cars are jammed.

ACKNOWLEDGMENTS

This work was supported by the State of North Rhine-Westphalia and by OTKA(T029985).

- [1] T.J. MacDonald, J.H. Gibbs, and A.C. Pipkin, *Biopolymers* **6**, 1 (1968).
- [2] B. Schmittmann and R.K.P. Zia, *Statistical Mechanics of Driven Diffusive Systems*, edited by C. Domb and J.L. Lebowitz (Academic Press, Orlando, 1995), Vol. 17.
- [3] T. Halpin-Healy and Y.C. Zhang, *Phys. Rep.* **254**, 214 (1995).
- [4] J.M.J. van Leeuwen and A. Kooiman, *Physica A* **184**, 79 (1992).
- [5] K. Nagel and M. Schreckenberg, *J. Phys. I* **2**, 2221 (1992).
- [6] M. Schreckenberg, A. Schadschneider, K. Nagel, and N. Ito, *Phys. Rev. E* **51**, 2939 (1995).
- [7] L.G. Tilstra and M.H. Ernst, *J. Phys. A* **31**, 5033 (1998).
- [8] A. Benyoussef, H. Chakib, and H. Ez-Zahraouy, *Eur. Phys. J. B* **8**, 275 (1999).
- [9] M.R. Evans, N. Rajewsky, and E.R. Speer, *J. Stat. Phys.* **95**, 45 (1999).
- [10] J. de Gier and B. Nienhuis, *Phys. Rev. E* **59**, 4899 (1999).
- [11] D. Chowdhury, L. Santen, and A. Schadschneider, *Phys. Rep.* **329**, 199 (2000).
- [12] N. Rajewsky, L. Santen, A. Schadschneider, and M. Schreckenberg, *J. Stat. Phys.* **92**, 151 (1998).
- [13] L.C.Q. Vilar and A.M.C. de Souza, *Physica A* **211**, 84 (1994).
- [14] G. Csányi and J. Kertész, *J. Phys. A* **28**, L427 (1995).
- [15] L. Roters, S. Lübeck, and K.D. Usadel, *Phys. Rev. E* **59**, 2672 (1999).
- [16] S. Lübeck, M. Schreckenberg, and K.D. Usadel, *Phys. Rev. E* **57**, 1171 (1998).
- [17] A. Schadschneider, *Eur. Phys. J. B* **10**, 573 (1999).
- [18] A. Schadschneider and M. Schreckenberg, *J. Phys. A* **26**, L679 (1993).
- [19] A. Schadschneider and M. Schreckenberg, *J. Phys. A* **30**, L69 (1997).
- [20] A. Schadschneider and M. Schreckenberg, *J. Phys. A* **31**, L225 (1998).
- [21] B. Eisenblätter, L. Santen, A. Schadschneider, and M. Schreckenberg, *Phys. Rev. E* **57**, 1309 (1998).
- [22] M. Sasvári and J. Kertész, *Phys. Rev. E* **56**, 4104 (1997).
- [23] L. Santen and A. Schadschneider, e-print cond-mat/9711261.
- [24] S. Cheybani, J. Kertész, and M. Schreckenberg, *J. Phys. A* **31**, 9787 (1998).
- [25] D. Chowdhury, J. Kertész, K. Nagel, L. Santen, and A. Schadschneider, *Phys. Rev. E* **61**, 3270 (2000).
- [26] S. Cheybani, J. Kertész, and M. Schreckenberg, preceding paper, *Phys. Rev. E* **63**, 016107 (2000).